

SUPPLEMENTAL MATERIAL

DETAILED METHODS

Myocardial Infarction

A total of 16 8-10-week-old mice were used, each weighing 24-28 g. Following block randomization, during which investigators were blinded to the allocation of animals to each group, a group of 8 mice underwent permanent occlusion of the left anterior coronary artery (MI group) as previously described,¹ and the remaining 8 mice were used as controls (No MI group). Power calculations were carried out to determine the necessary number of animals based on prior data ($p=0.05$; power=80%). Surgery was carried out under general anesthesia with 3-3.5% sevoflurane in 100% oxygen and providing mechanical ventilation, with a 200 μ l stroke volume and a rate of 200 strokes per minute. The heart was exposed by thoracotomy, and a 8/0 silk suture thread was passed under the left anterior coronary artery and knotted to occlude the artery 1 mm distal to the left atrial appendage. Thereafter, the chest wall was closed, and the skin was sutured with 6/0 nylon suture thread. Infarcted animals received analgesic treatment (0.1 mg/kg buprenorphine subcutaneously) for 3 to 5 days starting right after the surgery. Three days after surgery, transthoracic echocardiography was carried out to verify the successful of the procedure. Only those mice with 2 or more akinetic cardiac segments and a left ventricular ejection fraction below 45% were kept in the study for further analysis. All mice were euthanized 28 days after surgery.

Echocardiography

Transthoracic echocardiography was performed by an expert operator blinded to genotype and treatment using a high-frequency ultrasound system (Vevo 2100, Visualsonics) with a 40-MHz linear probe. Standard 2-dimensional (2D) and m-mode (MM) echography procedures were performed in long- and short-axis views (LAX and SAX, respectively) at a frame rate >230 frames/sec.² Mice were lightly anesthetized with 1-2% isoflurane in 100% oxygen, with isoflurane delivery adjusted to maintain a heart rate of 450-550 bpm. Mice were placed in a supine position on a heated platform set at 38.3°C, and warmed ultrasound gel was also used to maintain normal body temperature. A base apex electrocardiogram was monitored throughout anesthesia. Images were transferred to a computer and were analyzed off-line using the Vevo 2100 Workstation software (VisualSonic).

For the assessment of left ventricular (LV) systolic function, parasternal 2D long-axis views (LAX) were acquired. LV ejection fraction, LV end-diastolic volume, and LV end-systolic volume were obtained from this view using the area-length method. Changes in LV dimensions were evaluated from the MM SAX view, placing the line at the level of the papillary muscles. From this view, LV anterior and posterior wall thickness and cardiac mass were determined. As with the image acquisition, researchers were blinded to mouse genotype and treatment

iCLIP library preparation

Neonatal cardiomyocytes were extracted from C57BL/6 mice at P0 or P1 as described.¹ A total of 8 million cells were plated on 10 cm² plates. The following day, cells were transfected with 15 µg SRSF3-GFP modRNA using 21 µL Lipofectamine 2000. At 48 h post transfection, cells were irradiated once with 150 mJ/cm² UV light (254 nm) on ice and iCLIP was performed according to ³ with slight modifications. Crosslinked RNA was digested to lengths of 80-200 nucleotides using RNaseI (Ambion) at a 1:200 dilution, at 37°C for exactly 3 min in a thermomixer at 1,100 rpm. In order to reduce the RNA degradation, samples were treated with 2 µl of RNase Inhibitor (Promega), after the RNaseI treatment. RNA-protein complexes were immunopurified using Protein G Dynabeads® (ThermoFisher Scientific) coupled with a goat anti-GFP antibody (D. Drechsel, MPI-CBG, Dresden) by incubating the lysates and the beads in a rotating wheel for 1.5 h at 4°C. The 3' end of the RNAs was dephosphorylated using T4 PNK (NEB), at 37°C for 20 min in a thermomixer at 1,100 rpm. Isolated and purified RNA fragments were ligated using T4 RNA ligase (NEB) to pre-adenylated DNA 3' adapters (IDT) and their 5' ends were radio-labeled with P³²-γ-ATP (PerkinElmer). Samples were separated in a NuPAGE gel (Bio Rad) for 50 min at 180 V and transferred onto a nitrocellulose membrane for 2 h at 40 V. After RNA isolation from the membrane and treatment with proteinase K, isolated and purified RNA fragments were reverse-transcribed using barcoded RT-primers and SuperscriptIV (ThermoFisher Scientific). cDNA fragments were size-selected, circularized using CirLigaseTM (Epicentre) and re-linearized by *Bam*HI (NEB). The final cDNA libraries now containing 5' and 3' adapters were amplified using AccuPrime (ThermoFisher Scientific) and sequenced on an Illumina HiSeq2000 machine (single-end 75 nucleotide reads, 20 million reads per replicate).

Analysis of iCLIP data

Analysis of iCLIP sequencing data were done using iCount package (<http://icount.biolab.si>)

using default iCOUNT options. Briefly, adapters and barcodes were removed from all iCLIP reads before mapping to the mouse mm9 genome assembly (Ensembl65 annotation) using Bowtie (version 0.12.7). After analysis of reproducibility, replicates were pooled to allow determination of statistically significant cross-link events (X-links). For this, all uniquely mapping reads were used, PCR duplicates were removed using the random barcodes within the 3'adapter, X-link sites were extracted (1st nucleotide of the read) and randomized within co-transcribed regions. Significant X-links (false discovery rate [FDR] <0.05) were calculated using normalized numbers of input X-links as previously described.⁴⁻⁶ Bedfiles with significant X-link events were indexed with Tabix and intersected with event coordinates using pysam library to locate peaks within 250 bp of intronic and 100 bp exonic bases flanking each splice site concerning a particular splicing event (IR and CE). We selected for both analyses the closest upstream and downstream exon to the alternative exon, in order to simplify. Over-representation in each group was tested with a one-sided Fisher test. The same binding sites were then plotted relative to the exon cassette and intron retention coordinates using the starting position of the interval in the BED file. iCLIP data were deposited in Gene Expression Omnibus (GSE123002). The entire iCOUNT script for the analysis is available on github: <https://github.com/tomazc/iCount>

For motif searching, a Z-score analysis for enriched k-mers was performed as described previously.⁷ Sequences surrounding significant X-links were extended in both directions by 30 nucleotides (windows: -30 to -5 nt and 5-30 nt). All occurring k-mers within the evaluated interval were counted and weighed. Then a control dataset was generated by 100x randomly shuffling significant X-links within the same genes, and a Z-score was calculated relative to the randomized genomic positions. The top 20 k-mers were aligned to determine the *in vivo* binding consensus motif. Sequence logos were produced using WebLogo (<http://weblogo.berkeley.edu/logo.cgi>).

RNA isolation and qRT-PCR

RNA was isolated from the left ventricle or from isolated cells using TRIzol (15596026, Thermo Fisher Scientific). cDNA was synthesized from 100 ng of total RNA per sample using the Applied Biosystems High Capacity cDNA Reverse Transcription kit (4368814, Thermo Fisher Scientific). Quantitative PCR (qRT-PCR) was conducted with SYBR Green (4367659, Thermo Fisher Scientific), and cDNA was amplified using the primers listed in Online Table II. Results were analyzed using LinRegPCR.⁸ Values were normalized to GAPDH, SRSF3 exons 4-5, total expression of the corresponding mRNA, or F-Luc depending on the experiment, as indicated in the figures.

Immunofluorescence and immunohistochemistry

Hearts or embryos were extracted, fixed in 4% PFA, and embedded in paraffin. For immunofluorescence, 5 µm sections were unmasked with citrate solution, permeabilized with 0.3% Triton X-100 in PBS, and blocked with avidin-biotin (SP-2001, Vector Laboratories) when using anti-SRSF3 antibody. Sections were incubated with 10 µg/mL anti-SRSF3 (ab73891, Abcam) or anti-phospho-Histone H3 diluted 1:100 dilution (9701, Cell Signalling) and 4 µg/mL anti-TroponinT (MS295P, Thermo Fisher Scientific). Rabbit IgG and a mouse isotype-matching antibody were used as negative controls for anti-SRSF3 and anti-phospho-Histone H3, and for anti-TroponinT, respectively, to ensure the specificity of the signal. Nuclei were stained with DAPI (D1306, Thermo Fisher Scientific). After washing in PBS, sections were incubated with the following secondary antibodies as appropriate: biotinylated goat anti-rabbit (111-066-003, Jackson Immuno Research) plus streptavidin Cy3 (016-160-084, Jackson Immuno Research), Alexa 568-labeled goat anti-rabbit (A-11036, Thermo Fisher Scientific), or Alexa 488-labeled goat anti-mouse (A-11029, Thermo Fisher Scientific). Stained sections were mounted in Vectashield mounting medium (H-1000, Vector Laboratories).

Western blotting

Left ventricular myocardium was lysed in RIPA buffer in the presence of protease and phosphatase inhibitors (04693159001 and 04906845001, Roche Diagnostics).⁹ Lysates were separated by SDS-PAGE gels and transferred to PVDF membranes. Membranes were blocked with 3% skimmed milk in PBS or 5% BSA in TBS, depending on the antibody. The following primary antibodies were used: anti-SRSF3 (ab73891, Abcam), anti-SRSF1 (PA5-30220, Thermo Fisher Scientific), anti-vinculin (V4505, Sigma), anti-GAPDH (ab8245, Abcam), anti-SERCA2A (ab2861, Abcam), anti-MYH6/7 (ab90567, Abcam), anti-mTOR C-terminal (2983, Cell Signaling), anti-mTOR N-terminal (ab134903, Abcam), anti-AKT (4691, Cell Signaling), anti-Phospho-AKT (Ser473) (4058, Cell Signaling), anti-4E-BP1 (9644, Cell Signaling), anti-phospho-4E-BP1 (Ser65) (9451, Cell Signaling), and anti-phospho-4E-BP1 (Thr37/46) (9459, Cell Signaling). Secondary antibodies included anti-mouse P0447 and anti-rabbit P0448, both from Dako. Membranes were developed using ECL reagent (RPN2106, GE Healthcare Life Sciences). Brightness and contrast were adjusted linearly.

DNA constructs

Adeno-associated virus (AAV) constructs were made by cloning SERCA2A or luciferase between the CMV promoter and the SV40 polyA in a vector containing ITR sequences from AAV2. The human SERCA2A-coding sequence was a kind gift from Roger J. Hajjar.¹⁰ Constructs used to analyze mRNA stability were obtained from Franck Dequiedt's laboratory.¹¹ SRSF3 cDNA was cloned into the MS2-CP plasmid in the 3' region of MS2-CP. The SRSF3-GFP chimera was generated by inserting the SRSF3 cDNA into pEGFP-N1. Modified RNA (modRNA) cloning and production was as previously described.⁸

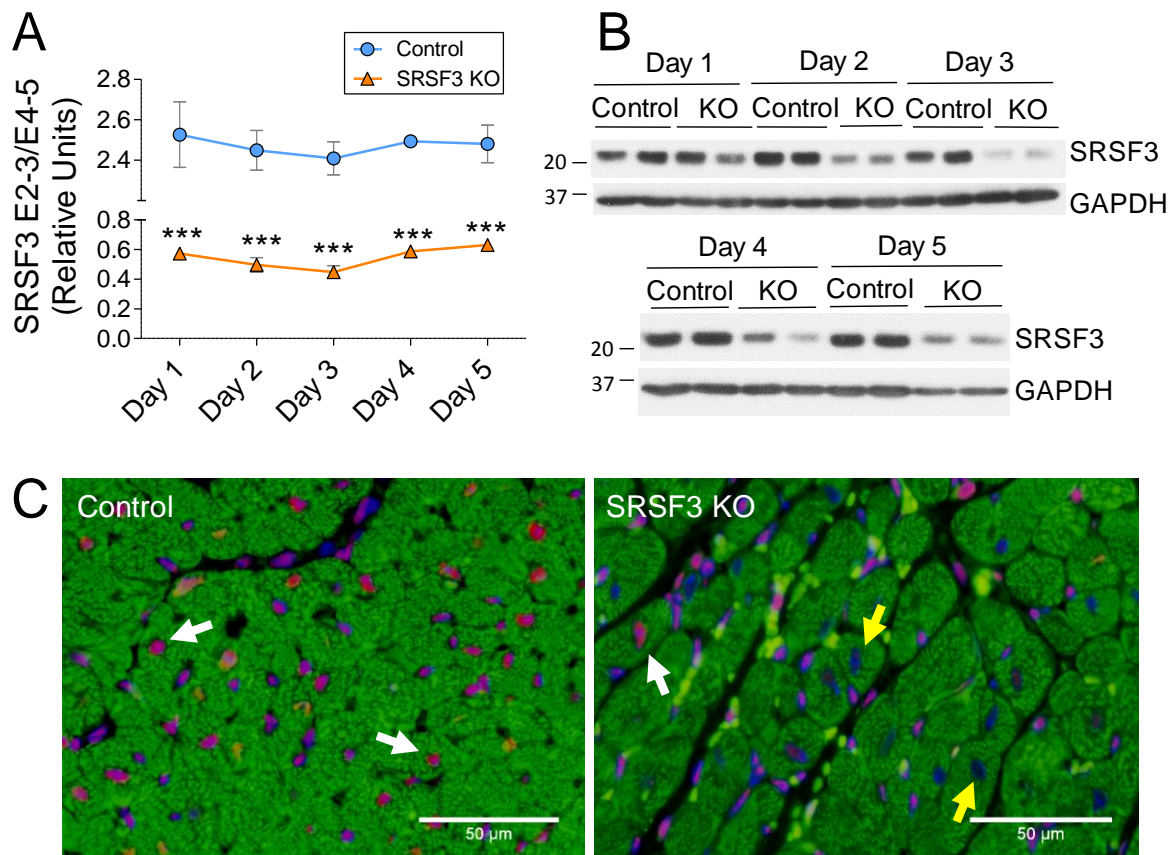
mRNA stability assay

mRNA stability was analyzed using an assay based on a protein-RNA binding system present in the MS2 virus.¹¹ This virus produces a coat protein (CP) that modulates viral RNA translation by binding to loop structures in the target mRNAs. To take advantage of this system, we used the plasmid Rluc8, which contains 8 of these loop repeats in the 3' region of *Renilla reniformis* luciferase (R-Luc). As a control, we used the same plasmid lacking these loop repeats (Rluc0). These reporter plasmids also express firefly luciferase (F-Luc) under the control of the same bidirectional promoter. Plasmids were co-transfected into P19 cells with expression plasmids for MS2-CP (control) or MS2-CP-SRSF3, which expresses SRSF3 fused to the 3' region of MS2-CP, thereby driving SRSF3 binding to transcripts that contain MS2-CP binding loops.¹¹ A total of 2 μ L of Lipofectamine 2000 (11668027, Thermo Fisher Scientific) and 0.5 μ g of each plasmid were used per well. At 48 h post-transfection, cells were treated with 10 μ g/mL actinomycin D (ActD) (A9415, Sigma) and collected at several time points after treatment. mRNA was analyzed by qRT-PCR using primers indicated in Online Table II. Luciferase activity was analyzed with the Dual-Luciferase Reporter Assay kit (E1980, Promega) in a Sirius Tube Luminometer (Berthold). R-Luc levels were normalized to F-Luc to avoid bias due to varying transfection efficiency.

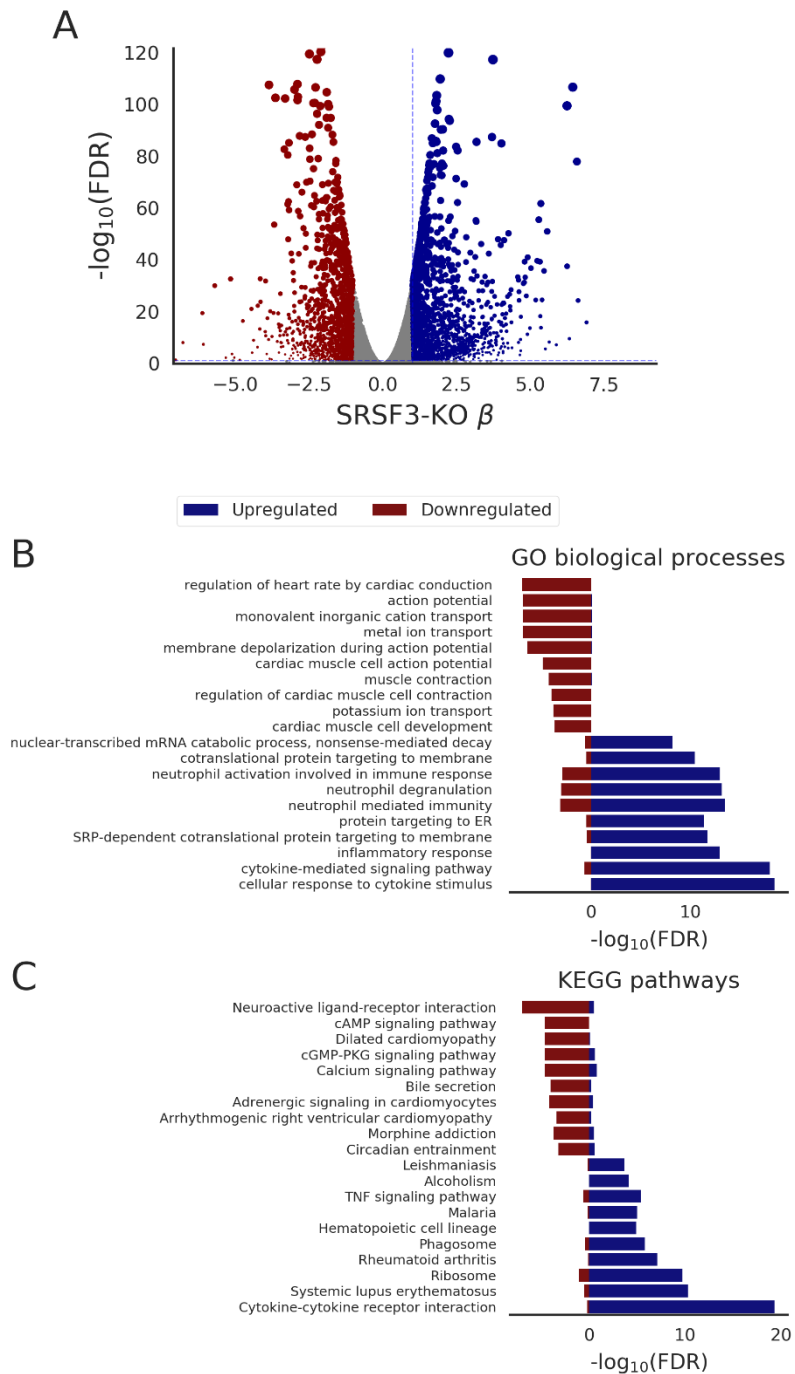
Adeno-associated virus production and injection

Adeno-associated virus was produced by the CNIC Viral Vectors Unit in HEK293 cells using serotype 9 capsid proteins. For viral administration, mice were anesthetized with 3-3.5% sevoflurane in 100% oxygen. A total of 50 μ L of saline (0.9% NaCl), containing 1×10^{11} VP/mL, were injected per mouse through the femoral vein in a single injection.

ONLINE FIGURES AND FIGURE LEGENDS

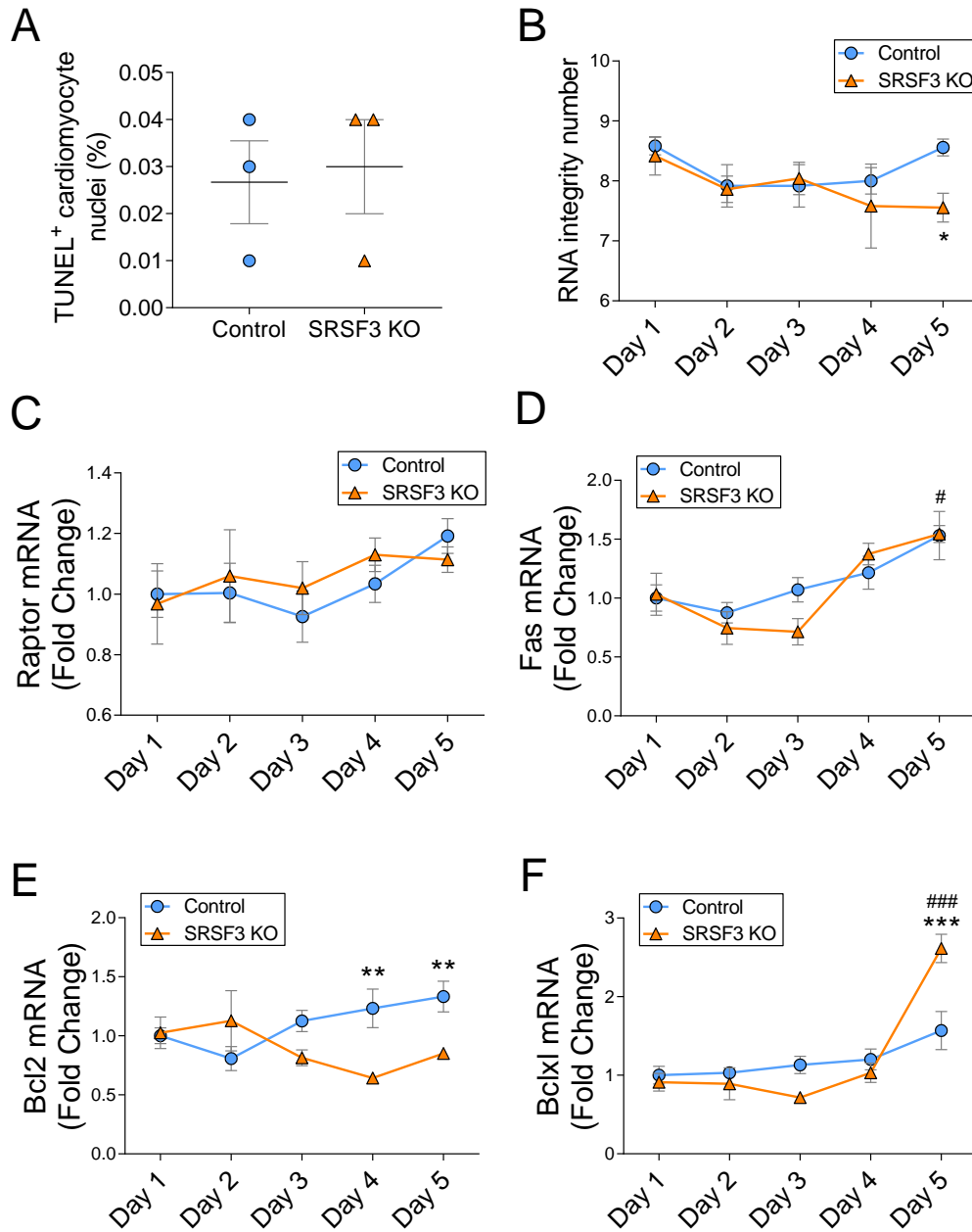


Online Figure I. SRSF3 KO mice lack SRSF3 expression specifically in cardiomyocytes. **A**, qRT-PCR analysis of the depletion in SRSF3 exons 2 and 3 in the heart over 5 days post tamoxifen induction. Data are shown as mean \pm SEM; $n=5-13$ mice per group. *** $p<0.001$ for SRSF3 KO vs Control; 2-way ANOVA followed by the Bonferroni post-test. **B**, Western blot analysis of SRSF3 protein expression in the heart over 5 days post tamoxifen induction. Molecular weight markers are indicated on the left. **C**, Immunofluorescence analysis with anti-SRSF3 (red), anti-TroponinT (green) and Dapi (blue) on heart sections from control and SRSF3 KO mice at day 5 post tamoxifen induction. Arrows indicate cardiomyocytes expressing SRSF3 (white) or recombination-positive cardiomyocytes lacking SRSF3 expression (yellow). Bar, 50 μ m.

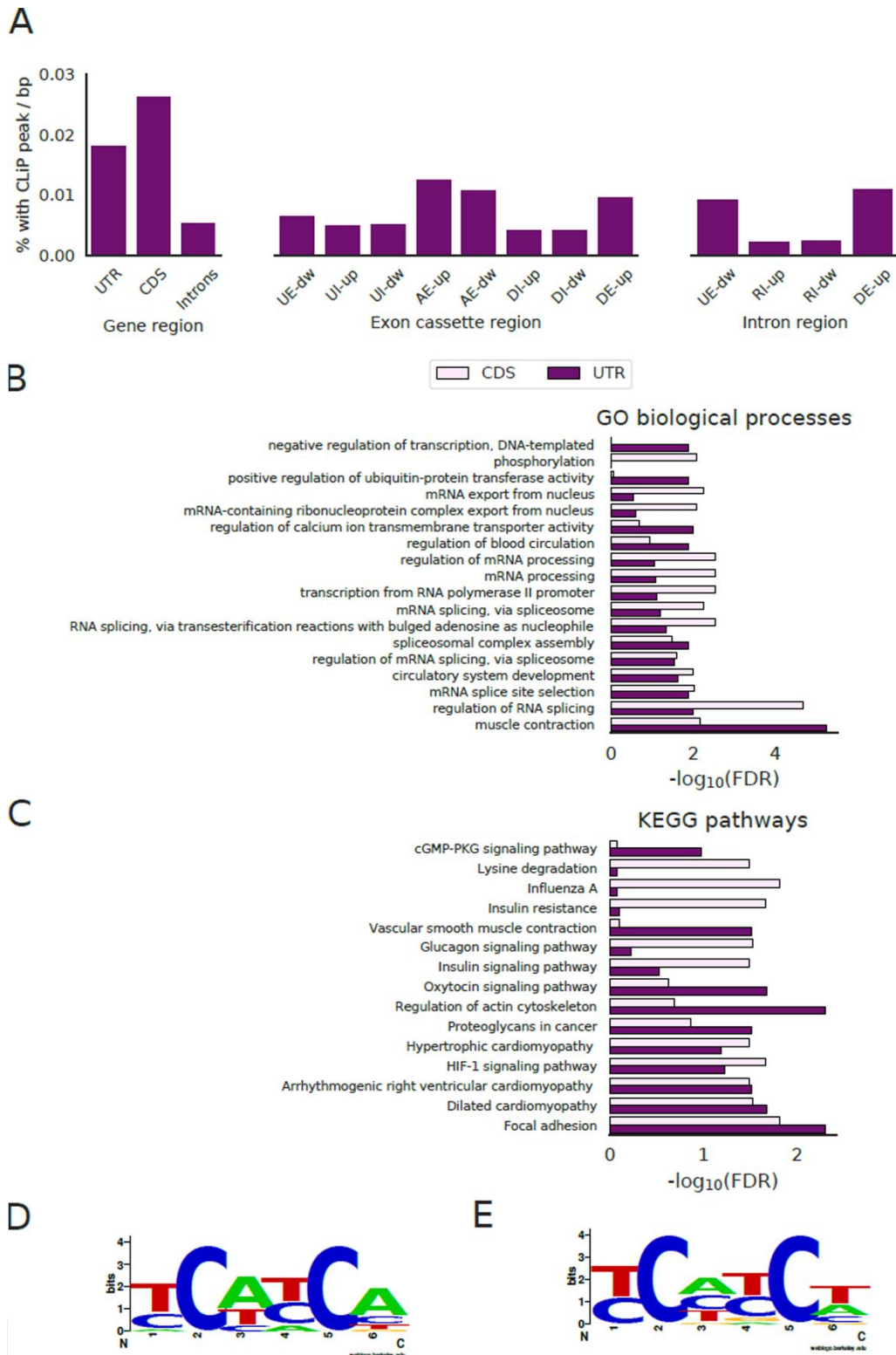


Online Figure II. SRSF3 depletion results in downregulation of contraction-related genes. **A**, Volcano plot representing results from differential gene expression analysis. The minus log transformation of the False Discovery Rate (FDR) is represented against the estimated Beta coefficient for the differences between SRSF3 KO and control mice using sleuth. Genes with an FDR lower than 0.05 and absolute Beta higher than 1 were considered to be differentially expressed. **B**, **C**, Enrichment analysis of up (shown in blue

towards the right) and down-regulated genes (red towards the left) upon SRSF3 depletion using Gene Ontology (GO) biological processes (B) and KEGG pathways (C) databases.

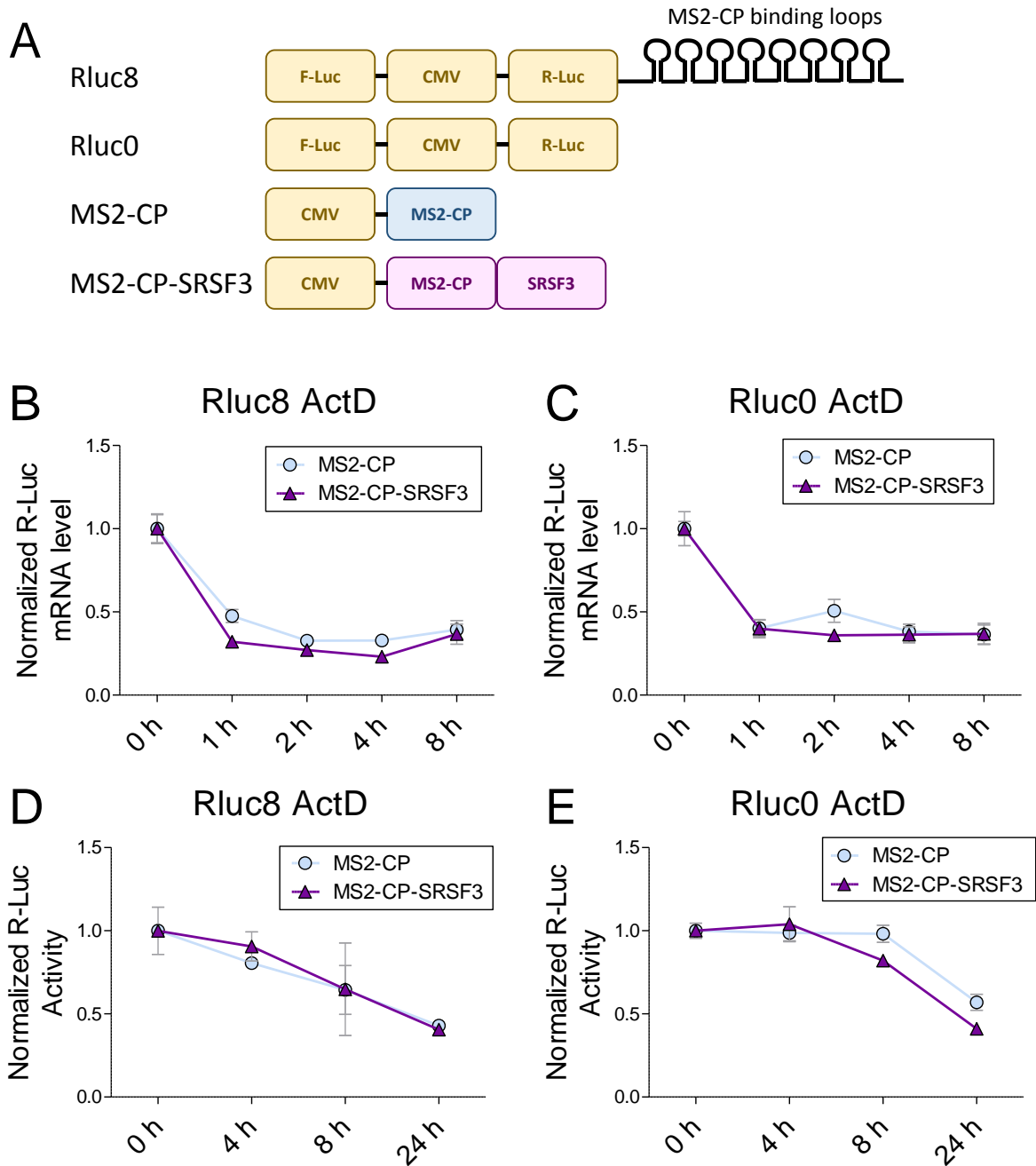


Online Figure III. SRSF3 KO mice show initial signs of apoptosis at late time points after tamoxifen injection. **A**, Percentage of apoptotic cardiomyocytes analyzed by TUNEL staining in control and SRSF3 KO mice 5 days after the last tamoxifen injection. **B**, RNA integrity number of total RNA from control and SRSF3 KO mice at different time points after the last tamoxifen injection. **C-F**, Raptor (C), Fas (D), Bcl2 (E) and Bclxl (F) mRNA expression in control and SRSF3 KO mice at different time points after the last tamoxifen injection. * $p < 0.05$, ** $p < 0.05$, *** $p < 0.01$ control vs SRSF3 KO mice; # $p < 0.05$, ### $p < 0.01$ vs day 1 post-tamoxifen. 2-way ANOVA plus Bonferroni's post-test. $n = 5-13$.

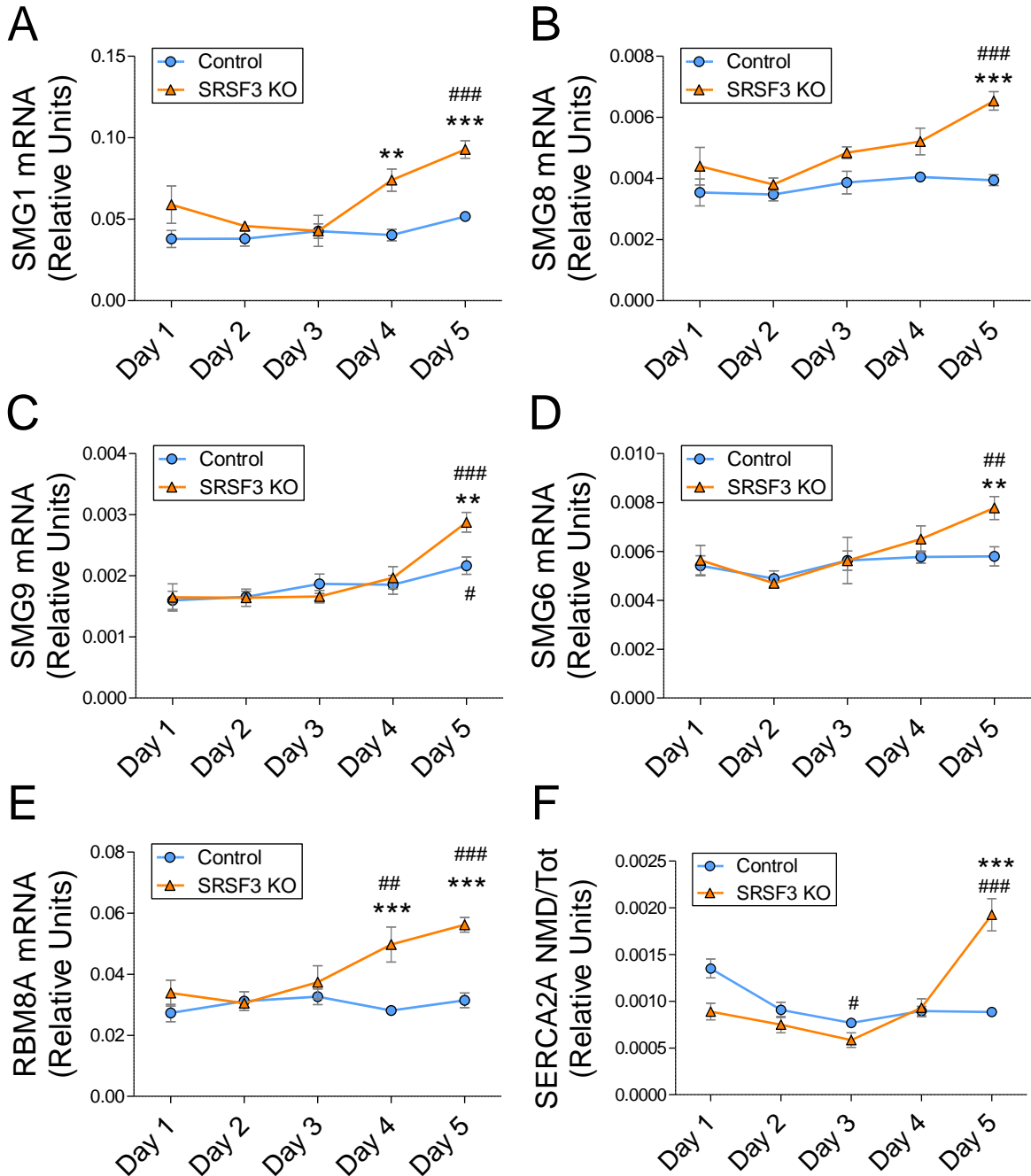


Online Figure IV. Individual-nucleotide resolution UV crosslinking and immunoprecipitation (iCLIP) analysis of SRSF3 binding in neonatal cardiomyocytes.

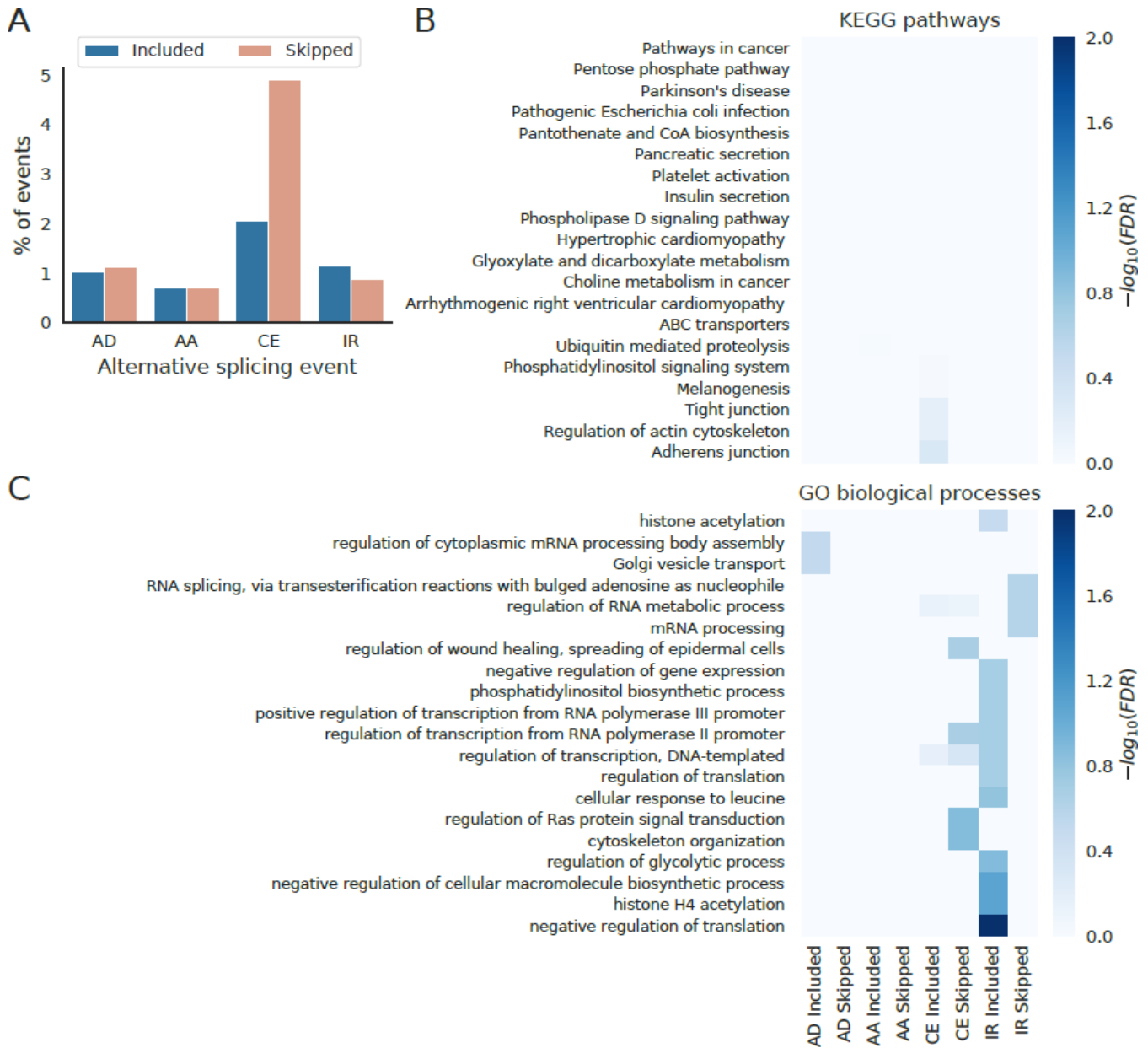
A. Percentage of genes (left), exon cassettes (center) or intron retention events (right) with binding sites in each specified region divided by the total length of the region that was analyzed UE, Upstream exon; RI, Retained Intron; DE, Downstream exon; AE, Alternative exon; UI, Upstream Intron; DI, Downstream Intron; up: upstream flank; dw, downstream flank; CDS, coding exons; UTR, untranslated region; Intron, intronic regions. **B, C.** Functional enrichment analyses using GO (B) and KEGG (C) databases for genes with iCLIP peaks in either UTR or CDS regions compared with genes detected to be expressed in the RNA-Seq data. **D, E.** Consensus motifs for SRSF3 identified in iCLIP peaks in all regions of the mRNA (D) and in the UTRs alone (E).



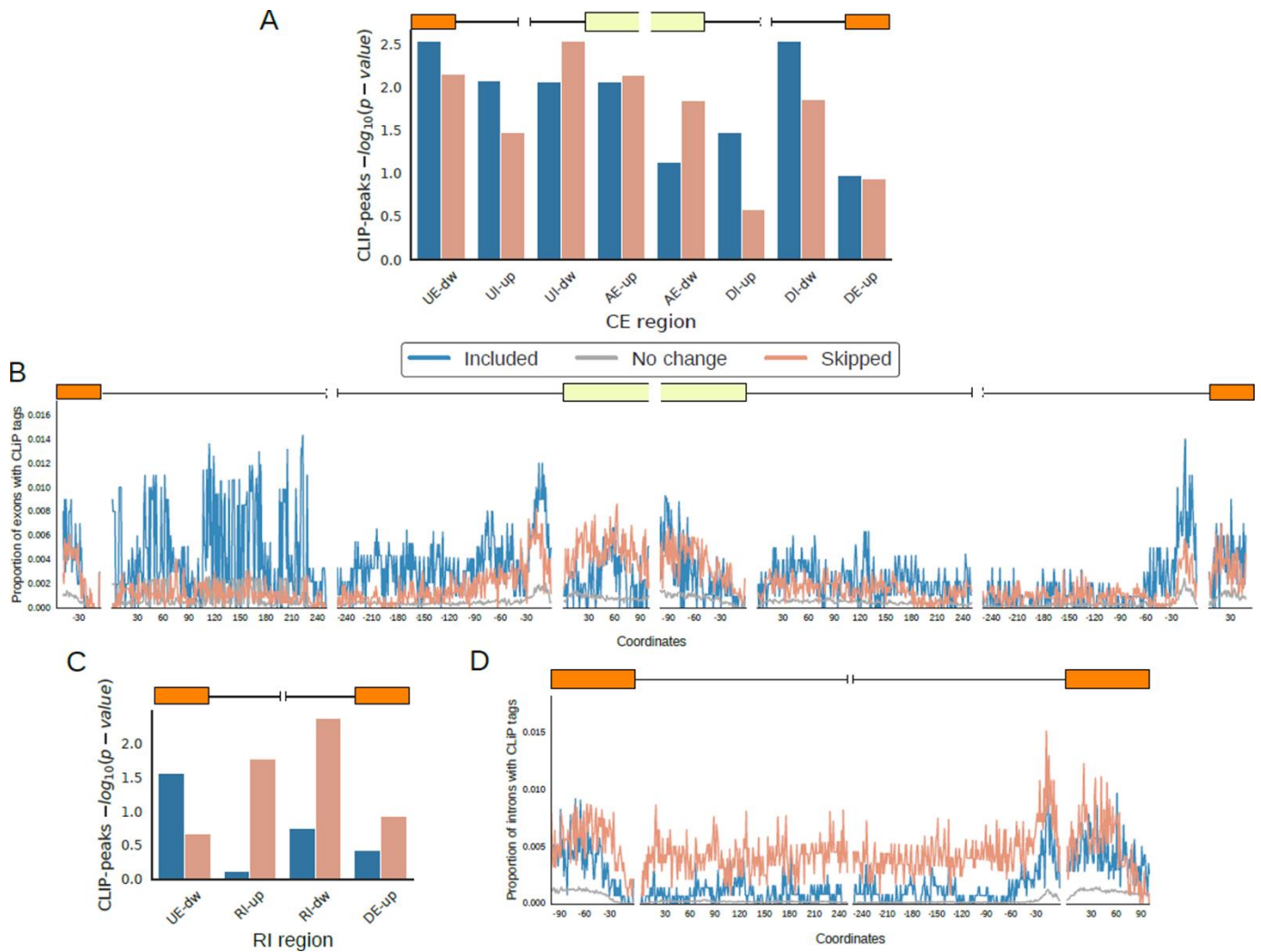
Online Figure V. SRSF3 binding to the 3' UTR does not increase mRNA stability. A, Plasmids used for mRNA stability assay. P19 cells were transfected with MS2-CP or MS2-CP-SRSF3 and Rluc8 or Rluc0. Rluc8 contains 8 repeats of the MS2-CP binding loop in the 3'UTR region of R-Luc, whereas Rluc0 contains no loops (control). After transfection, cells were treated with actinomycin D (ActD) and R-Luc mRNA expression and enzyme activity were monitored for several hours. **B, C,** qRT-PCR analysis of R-Luc mRNA expression in cells transfected with Rluc8 and Rluc0 plasmids. **D, E,** R-Luc enzyme activity in cells transfected with Rluc8 and Rluc0 plasmids. Data are shown as mean \pm SEM; n=3-5 per group. 2-way ANOVA followed by the Bonferroni post-test.



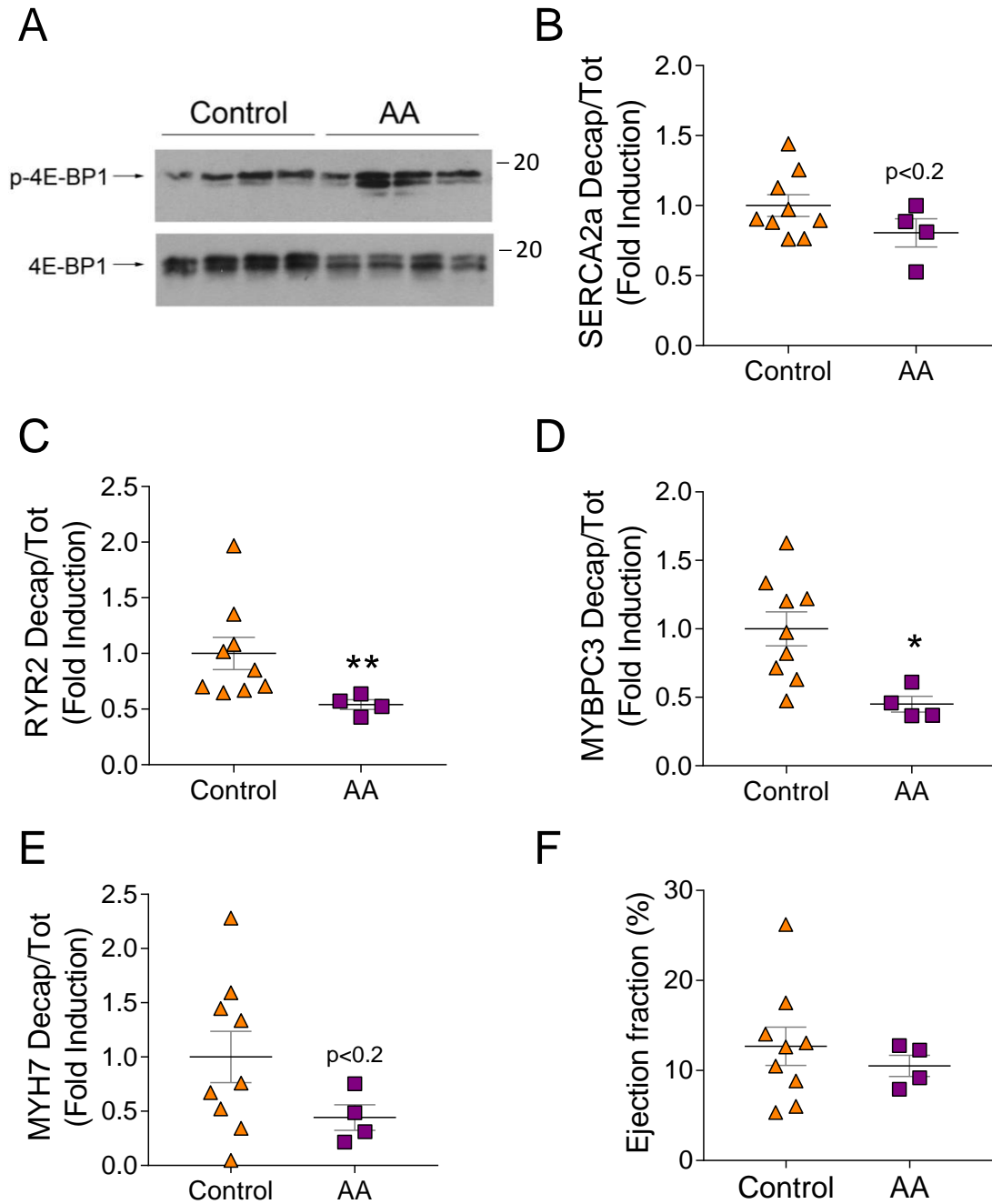
Online Figure VI. SRSF3 depletion leads to a late induction of non-sense mediated decay (NMD). A-E, qRT-PCR analysis of the cardiac expression of SMG1 (A), SMG8 (B), SMG9 (C), SMG6 (D), and RBM8A (E) in control and SRSF3 KO hearts over 5 days post tamoxifen induction. F, qRT-PCR analysis of cardiac SERCA2A NMD isoform expression in control and SRSF3 KO hearts over 5 days post tamoxifen induction; expression was normalized to total SERCA2A. Data are shown as mean \pm SEM; n=5-13 per group. **p<0.01, ***p<0.001 for SRSF3 KO vs control; ##p<0.01, ###p<0.001 vs Day 1; 2-way ANOVA followed by the Bonferroni post-test.



Online Figure VII. Alternative splicing changes in cardiac-specific SRSF3 KO mice. A. Percentage of events showing increased (Included) and decreased (Skipped) inclusion rates in the SRSF3-KO mice according to the type of event (AD: Alternative Donor; AA: Alternative Acceptor; CE: Cassette Exon; IR: Intron Retention). **B, C.** Enrichment analysis of differentially spliced genes using KEGG pathways (B) and Gene Ontology (GO) biological processes (C) databases.



Online Figure VIII. Distribution of SRSF3 iCLIP peaks in alternatively spliced exons and introns in SRSF3 KO mice. **A**, Significance of the enrichment of iCLIP peaks in AS events showing differential inclusion in SRSF3 KO mice depending on the region of binding for Cassette Exons (CE). UE: Upstream exon; DE: Downstream exon; AE: Alternative exon; UI: Upstream Intron; DI: Downstream Intron; up: upstream flank; dw: downstream flank. **B**, Proportion of events with iCLIP tags in regions flanking the splicing sites of alternatively spliced cassette exons. The coordinates indicate the number of nucleotides upstream or downstream the splicing site. **C**, Significance of the enrichment of iCLIP peaks in AS events showing differential Intron Retention (IR). UE: Upstream exon; RI: Retained Intron; DE: Downstream exon. **D**, Proportion of events with iCLIP tags in regions flanking the splicing sites of retained introns.



Online Figure IX. mTOR stimulation decreases mRNA decapping of some sarcomeric genes. **A-E**, Mice were injected with an amino acid solution (AA) to activate mTOR starting at day 2 of tamoxifen treatment. Mice were sacrificed 5 days after the last tamoxifen injection and 4E-BP1 phosphorylation (T37/46) (**A**), decapped and total mRNA (**B-E**) were analysed. Note that the control (untreated) animals for these analyses are those shown in Fig. 5 (day 5), and are repeated here for comparative purposes. qRT-PCRs of control and treated animals were run and analysed together. **F**, Ejection fraction was analysed by echocardiography 5 days after the last tamoxifen injection before sacrificing the animals. *p<0.05 student's parametric t-test (**B**, **D-F**); **p<0.01 Mann-Whitney (**C**). n=4-9.

ONLINE TABLES**Online Table I. Sequences for mouse genotyping primers (5'-3')**

Name	Sequence
X16X3i	GCGCAGGTA CTTGAGAGA
Xi3Ri	CCCTTTTATTGGTCAGTGA
Cre Fw	TGACGGTGGGAGAATGTTAAT
Cre Rv	GCCGTAAATCAATCGATGAGT
mER-Cre-mER Fw	CTAGGCCACAGAATTGAAA
mER-Cre-mER Rv	GTAGGTGGAAATTCTAGCA

Online Table II. SYBR Green primer sequences used for qRT-PCR (5'-3').

Gen	Forward	Reverse
SRSF3	TCGTCGTCCTCGAGATGATT	CTCCTTCTTGGGGATCTGC
GAPDH	CTGCACCACCAACTGCTTAG	AGATCCACGACGGACACATT
SRSF3 NMD	TGGAAGTGTGAATGGTGAA	GACGCTGAAAGGGCTAGTTG
SRSF3 E2-3	ATCGTGATTCCTGTCCCTTG	TTCACCATTTCGACAGTTCCA
SRSF3 E4-5	ATCCCAAGAAGGAGAAGC	ATCGAGACGGCTTGTGATTT
BNP	GCCAGTCTCCAGAGCAATTC	TCTTTTGTGAGGCCTTGGTC
Acta1	CCAGAGTCAGAGCAGCAGAA	CAAAGCCAGCTTTCACCAG
SERCA2A	GAGGAAGGGGAAGAAACGAT	TCGATACACTTTGCCATTTC
RyR2	CCGGTCTTCCACTGACAAAC	GAGGACACGCTGACCAAGAT
MYBPC3	GGTCAAGATTGACTTTGTGCCTA	CAGACCACAGTGGGAGCAG
TNNT2	GCGGAAGAGTGGGAAGAGACAGAC	GCACGGGGCAAGGACACAAG
MYH7	CAACTGGAGGAGGAGGTCAA	CCTCTGTATGGCATCCGTCT
MYH6	ATGTTAAGGCCAAGGTCGTG	GTAGCGCTCCTTGAGGTTGT
TNNI3	GAAGCAGGAGATGGAACGAG	TGACTTTTGCTTCCACGTCA
R-Luc	TCTTTTTCGCAACGGGTTT	GCCCAGTTTCTATTGGTCTCC
F-Luc	TGAGAACTTCAGGCTCCTGG	GCCTTATGCAGTTGCTCTCC
rP5_RND	CTTCCCTACACGACGCTCTTCCGATrCrUrNrNrNrNrNrNrNrN	
SERCA2A Decap	CTACACGACGCTCTTCCGAT	AGCCCCTCAGCTCTGCAC
RyR2 Decap		GTGAGGACGCAGGGAGGA
MYBPC3 Decap		TACTTGTCATTGGCGGTGAT
MYH7 Decap		CAGCTCCCACTCCTACCTGA
SMG1	TCTGCGAAAGATGAGGTGAA	AACGAGCCACCAAAGAATG
SMG8	AACCCTCCTGTGCTCTACCA	TGATCCAATTTCCCACAACA
SMG9	CCTGGGCTCTACGGGATAG	GAGAGGATGATGGGGGTTTT
SMG6	CCCCAGTGTGAAAGTCTGGT	AGGGTGAGGTCATCATCTGG
RBM8A	TGTCACTGGAGTCCACGAAG	CACCAGTCCCACTGATTGG
SERCA2A NMD	TGTTTTCTCCAATGCCTTC	CTTTTCCCAACCTCAGTCA

Online Table III. Loss of SRSF3 leads to severe contraction defects

		Basal		Day 5	
		Control	SRSF3 KO	Control	SRSF3 KO
2D	LVEF (%)	65.72±3.69	64.25±3.04	57.62±2.83	12.68±2.13 ^{*****}
	LVESV (µl)	17.93±3.55	21.89±4.16	25.48±4.85	56.83±3.32 ^{*****}
	LVEDV (µl)	51.33±4.78	59.82±6.13	58.98±7.56	65.39±7.98
MM	AWd (mm)	0.81±0.05	0.72±0.03	0.78±0.05	0.68±0.06
	PWd (mm)	0.63±0.03	0.69±0.05	0.70±0.03	0.69±0.05
	FS (%)	38.1±4.11	35.24±0.71	31.3±2.21	7.61±1.7 ^{###}
	LVMc	67.55±2.83	72.51±6.12	79.28±3.96	75.7±8.45
	n	3	5	6	9

Control and SRSF3 KO mice were treated with tamoxifen (see Methods). Echocardiography analysis was performed before treatment and on day 5 day after treatment. Data are mean values ±SEM.

AWd, anterior wall diastolic thickness; FS, fractional shortening; LVEDV, left ventricular end diastolic volume; 2D, two-dimensional; MM, motion-mode; LVEF, left ventricular ejection fraction; LVESV, left ventricular end systolic volume; LVMc, left ventricle mass corrected; PWd, posterior wall diastolic thickness.

*p<0.05, ***p<0.001 for SRSF3 KO vs Control. ##p<0.01, ###p<0.001 Day 5 vs Basal; 2-way ANOVA followed by the Bonferroni post-test.

Online Table IV (see online dataset). Differential gene expression analysis using kallisto and sleuth, indexed by gene id with the corresponding associated gene symbol. "b" is the beta coefficient resulting from Wald test, related to the log transformation of the fold change. "se_b" is the estimated standard error of "b". "p-value" represents the raw p-value of the contrast, which was corrected for multiple testing in the column "q-value".

Online Table V. SERCA2A overexpression partially rescues contraction defects in SRSF3 KO mice

		AAV-LUC		AAV-SERCA2A	
		Control	SRSF3 KO	Control	SRSF3 KO
2D	LVEF (%)	60.82±1.59	9.57±1.32***	57.65±1.85	15.98±1.57***#
	LVESV (µl)	18.33±1.92	64.22±3.44***	26.01±3.25	63.46±4.87***
	LVEDV (µl)	45.57±3.59	71.15±4.14***	60.68±5.27	75.23±4.93
MM	AWd (mm)	0.84±0.06	0.73±0.04	0.73±0.02	0.75±0.03
	PWd (mm)	0.75±0.02	0.79±0.03	0.83±0.07	0.78±0.04
	FS (%)	40.17±2.15	5.77±1.21***	32.98±2.18#	6.15±1.39***
	LVMc	76.22±3.33	88.46±8.17	83.71±5.80	98.10±3.95
	n	8	8	7	10

Control and SRSF3 KO mice were administered AAV-SERCA2A or AAV-LUC and then treated with tamoxifen (see Methods). Echocardiography analysis was performed on day 5 day after tamoxifen induction. Data are mean values ±SEM.

AWd, anterior wall diastolic thickness; FS, fractional shortening; LVEDV, left ventricular end diastolic volume; 2D, two dimensional; MM, motion-mode; LVEF, left ventricular ejection fraction; LVESV, left ventricular end systolic volume; LVMc, left ventricle mass corrected; PWd, posterior wall diastolic thickness.

***p<0.001 for SRSF3 KO vs Control. #p<0.05 for AAV-SERCA2A vs AAV-LUC; 2-way ANOVA followed by the Bonferroni post-test.

Online Table VI (see online dataset). mRNAs with iCLIP binding sites. iCLIP peaks in untranslated regions (UTR), coding sequence (CDS) and introns were identified for those genes that showed differential expression. "1" represents SRSF3 binding to that region in the gene, whereas "0" means there were no SRSF3 peaks identified in that region.

Online Table VII (see online dataset). Results of differential splicing analysis using vast-tools. "EVENT": Vast-tools event id. "SRSF3 cKO": estimated percent spliced in (PSI) in the SRSF3 cardiac-specific KO mice. "Control", PSI in the control mice. "dPSI", estimate difference in PSI between SRSF3 cKO and Control mice. " $P(|dPsi| > x) > 0.95$ ", difference in inclusion rate for which there is a 95% probability that the real absolute differences between genotypes is higher than that value. Values higher than 0 represent significantly changed events. "COORD" represents the coordinates of the splicing event as given by vast-tools.

Online Table VIII (see online dataset). Number of iCLIP binding sites for each exon skipping event for different regions in the event. "event_id": Vast-tools event id. Genomic coordinates are indicated. Region codes: UE, Upstream exon; DE, Downstream exon; AE, Alternative exon; UI, Upstream Intron; DI, Downstream Intron; up, upstream flank; dw, downstream flank. Intronic regions were 250 bp long and exonic regions 100 bp long.

Online Table IX (see online dataset). Number of iCLIP binding sites for each intron retention event for different regions in the event. "event_id", Vast-tools event id. Genomic coordinates are indicated. Region codes: UE, Upstream exon; RI, Retained Intron; DE, Downstream exon; up: upstream flank; dw: downstream flank. Intronic regions were 250 bp long and exonic regions 100 bp long.

SUPPLEMENTAL REFERENCES

1. López-Olañeta MM, Villalba M, Gómez-Salineró JM, Jiménez-Borreguero LJ, Breckenridge R, Ortiz-Sánchez P, García-Pavía P, Ibáñez B, Lara-Pezzi E. Induction of the calcineurin variant CnA β 1 after myocardial infarction reduces post-infarction ventricular remodelling by promoting infarct vascularization. *Cardiovasc Res*. 2014;102:396-406.
2. Padrón-Barthe L, Villalba-Orero M, Gómez-Salineró JM, Acín-Pérez R, Cogliati S, López-Olañeta M, Ortiz-Sánchez P, Bonzón-Kulichenko E, Vázquez J, García-Pavía P, Rosenthal N, Enríquez JA, Lara-Pezzi E. Activation of Serine One-Carbon Metabolism by Calcineurin A β 1 Reduces Myocardial Hypertrophy and Improves Ventricular Function. *J Am Coll Cardiol*. 2018;71:654-667.
3. Huppertz I, Attig J, Ambrogio AD, Easton LE, Sibley CR, Sugimoto Y, Tajnik M, König J, Ule J. iCLIP : Protein – RNA interactions at nucleotide resolution. *Methods*. 2014;65:274-287.
4. Yeo GW, Coufal NG, Liang TY, Peng GE, Fu X, Gage FH. An RNA code for the FOX2 splicing regulator revealed by mapping RNA-protein interactions in stem cells. *Nat Struct Mol Biol*. 2009;16:130-137.
5. König J, Zarnack K, Rot G, Curk T, Kayikci M, Zupan B, Turner DJ, Luscombe NM, Ule J. iCLIP reveals the function of hnRNP particles in splicing at individual nucleotide resolution. *Nat Struct Mol Biol*. 2010;17:909-916.
6. Wang Z, Kayikci M, Briese M, Zarnack K, Luscombe NM, Rot G, Ule J. iCLIP Predicts the Dual Splicing Effects of TIA-RNA Interactions. *PLoS Biol*. 2010;8.
7. Botti V, Mcnicoll F, Steiner MC, Richter FM, Solovyeva A, Wegener M, Schwich OD, Poser I, Zarnack K, Wittig I, Neugebauer KM, Mcnicoll MM. Cellular differentiation state modulates the mRNA export activity of SR proteins. *J Cell Biol*. 2017:1-17.
8. Gómez-Salineró JM, López-Olañeta MM, Ortiz-Sánchez P, Larrasa-Alonso J, Gatto A, Felkin LE, Barton PJR, Navarro-Lérida I, Ángel del Pozo M, García-Pavía P, Sundararaman B, Giovinazo G, Yeo GW, Lara-Pezzi E. The Calcineurin Variant CnA β 1 Controls Mouse Embryonic Stem Cell Differentiation by Directing mTORC2 Membrane Localization and Activation. *Cell Chem Biol*. 2016;23:1372-1382.
9. Felkin LE, Narita T, Germack R, Shintani Y, Takahashi K, Sarathchandra P, López-Olañeta MM, Gómez-Salineró JM, Suzuki K, Barton PJR, Rosenthal N, Lara-Pezzi E. Calcineurin splicing variant calcineurin A β 1 improves cardiac function after myocardial

- infarction without inducing hypertrophy. *Circulation*. 2011;123:2838-2847.
10. Goonasekera SA, Lam CK, Millay DP, Sargent MA, Hajjar RJ, Kranias EG, Molkenin JD. Mitigation of muscular dystrophy in mice by SERCA overexpression in skeletal muscle. *J Clin Invest*. 2011;121:1044-1052.
 11. Rambout X, Detiffe C, Bruyr J, et al. The transcription factor ERG recruits CCR4-NOT to control mRNA decay and mitotic progression. *Nat Struct Mol Biol*. 2016;23:663-672.

LEGENDS FOR VIDEO FILES

Online Video I. Parasternal 2D long axis echocardiography view of control and SRSF3 KO mice 5 days after tamoxifen induction.